

## Experimental Demonstration of Inequivalent Mutually Unbiased Bases

Wen-Zhe Yan,<sup>1,2,\*</sup> Yunting Li,<sup>3,4,5,\*</sup> Zhibo Hou,<sup>1,2,6,†</sup> Huangjun Zhu,<sup>3,4,5,‡</sup> Guo-Yong Xiang<sup>Ⓞ,1,2,6,§</sup>  
Chuan-Feng Li,<sup>1,2,6</sup> and Guang-Can Guo<sup>1,2,6</sup>

<sup>1</sup>CAS Key Laboratory of Quantum Information, University of Science and Technology of China,  
Hefei 230026, People's Republic of China

<sup>2</sup>CAS Center For Excellence in Quantum Information and Quantum Physics, University of Science and Technology of China,  
Hefei 230026, People's Republic of China

<sup>3</sup>State Key Laboratory of Surface Physics and Department of Physics, Fudan University, Shanghai 200433, China

<sup>4</sup>Institute for Nanoelectronic Devices and Quantum Computing, Fudan University, Shanghai 200433, China

<sup>5</sup>Center for Field Theory and Particle Physics, Fudan University, Shanghai 200433, China

<sup>6</sup>Hefei National Laboratory, University of Science and Technology of China, Hefei 230088, People's Republic of China



(Received 23 September 2023; accepted 12 January 2024; published 21 February 2024)

Quantum measurements based on mutually unbiased bases (MUBs) play crucial roles in foundational studies and quantum information processing. It is known that there exist inequivalent MUBs, but little is known about their operational distinctions, not to say experimental demonstration. In this Letter, by virtue of a simple estimation problem, we experimentally demonstrate the operational distinctions between inequivalent triples of MUBs in dimension 4 based on high-precision photonic systems. The experimental estimation fidelities coincide well with the theoretical predictions with only 0.16% average deviation, which is 25 times less than the difference (4.1%) between the maximum estimation fidelity and the minimum estimation fidelity. Our experiments clearly demonstrate that inequivalent MUBs have different information extraction capabilities and different merits for quantum information processing.

DOI: [10.1103/PhysRevLett.132.080202](https://doi.org/10.1103/PhysRevLett.132.080202)

*Introduction.*—Quantum measurements play a key role in extracting information from quantum systems and in achieving various quantum information processing tasks, such as quantum computation, quantum communication, quantum metrology, quantum sensing, and quantum simulation [1–3]. Rank-1 projective measurements are the simplest quantum measurements discussed in most elementary textbooks on quantum mechanics. Nevertheless, their properties become elusive if we consider two or more projective measurements. Since each rank-1 projective measurement is tied to an orthonormal basis, and vice versa, the study of rank-1 projective measurements is intertwined with the study of orthonormal bases.

Two rank-1 projective measurements are *mutually unbiased* or complementary if the outcome of one measurement is completely random whenever the outcome of the other measurement is certain. The corresponding bases are *mutually unbiased bases* (MUBs) [4–7]. MUBs are closely tied to the complementarity principle [8] and uncertainty relations [9–13], which play key roles in quantum mechanics. Moreover, they have numerous applications in quantum information processing, including quantum cryptography [7,13–16], quantum random access codes [17,18], quantum state estimation [5,6,19–21], quantum verification [22,23], and entanglement detection [24–26]. MUBs can be constructed using various interesting objects, including finite fields [5–7], mutually

unbiased Hadamard matrices [7,27], mutually orthogonal Latin squares [28], and symplectic spreads [29]. Except for prime-power dimensions, however, it is still a major open problem to determine the maximum number of bases in MUBs, even in dimension 6 [30].

Two sets of MUBs are (unitarily) *equivalent* if they can be turned into each other by unitary transformations up to the order of basis elements and overall phase factors. Otherwise, they are *inequivalent*. Inequivalent MUBs exist in certain dimensions of at least 4 [27], and this intriguing phenomenon has attracted the attention of many researchers in various research areas [7,16–18,27,29,31–33]. However, little is known about the operational distinctions between inequivalent MUBs, and there is no experimental demonstration before as far as we know.

As notable exceptions, Aguilar *et al.* showed that inequivalent MUBs can achieve different success probabilities in quantum random access codes [17]. Designolle *et al.* showed that inequivalent MUBs may have different degrees of measurement incompatibility as quantified by the noise robustness [31]. Hiesmayr *et al.* showed that some MUBs are more effective than others in detecting entanglement [32]. It is not clear whether these results can be demonstrated in experiments in the near future. Very recently, starting from a simple estimation problem, one of the authors showed that inequivalent MUBs may have different information-extraction capabilities and can be

distinguished by the *estimation fidelity* [33], which is amenable to experimental demonstration.

In this Letter, using photonic systems, we experimentally demonstrate the operational distinctions between inequivalent triples of MUBs in dimension 4 based on a simple three-copy estimation problem. To this end, we use polarization and path degrees of freedom of a photon to form a ququad. Then we implement a three-copy estimation protocol in which the projective measurements are determined by triples of MUBs, so that the estimation fidelities are tied to the intrinsic properties of MUBs. Notably, we can implement each projective measurement in one shot instead of simulating each basis-state projection sequentially as in previous experiments on high-dimensional MUBs [34–36]. The projective measurements we realized have average fidelity above 0.995. The experimental estimation fidelities coincide well with the theoretical predictions with only 0.16% average deviation, which is 25 times less than the difference (4.1%) between the maximum estimation fidelity and the minimum estimation fidelity. In this way, our experiments clearly demonstrate different information-extraction capabilities of inequivalent MUBs, which has never been demonstrated before.

*A simple estimation problem.*—Suppose a device can prepare  $N$  copies of a random pure quantum state  $\rho$  on a  $d$ -dimensional Hilbert space  $\mathcal{H}$  according to the Haar measure. We are asked to estimate the identity of  $\rho$  as accurately as possible as quantified by the average fidelity. If we perform the quantum measurement characterized by the positive operator-valued measure (POVM)  $\mathcal{A} = \{A_j\}_j$  on  $\rho^{\otimes N}$ , then the probability of obtaining outcome  $A_j$  is  $p_j = \text{tr}(\rho^{\otimes N} A_j)$ . Let  $\hat{\rho}_j$  be the estimator corresponding to outcome  $j$ . Let  $P_{N+1}$  be the projector onto the symmetric subspace in  $\mathcal{H}^{\otimes(N+1)}$  and  $D_{N+1} = \text{tr}(P_{N+1})$ . Then the average fidelity reads [33]

$$\begin{aligned} \bar{F} &= \sum_j \int d\rho p_j \text{tr}(\rho \hat{\rho}_j) = \frac{\sum_j \text{tr}[\mathcal{Q}(A_j) \hat{\rho}_j]}{(N+1)! D_{N+1}} \\ &\leq F(\mathcal{A}) := \sum_j \frac{\|\mathcal{Q}(A_j)\|}{(N+1)! D_{N+1}}, \end{aligned} \quad (1)$$

where the integration is over all pure states and

$$\mathcal{Q}(A_j) := (N+1)! \text{tr}_{1,\dots,N} [P_{N+1}(A_j \otimes \mathbb{1})]. \quad (2)$$

The upper bound in Eq. (1) is saturated if and only if each estimator  $\hat{\rho}_j$  is supported in the eigenspace of  $\mathcal{Q}(A_j)$  associated with the largest eigenvalue. Here,  $F(\mathcal{A})$  is the maximum average fidelity that can be achieved by the POVM  $\mathcal{A}$  and is called the *estimation fidelity* [33]. It is invariant under unitary transformations of the form  $U^{\otimes N}$  and thus encodes valuable information about the intrinsic properties of the POVM  $\mathcal{A}$ . It is pretty useful for

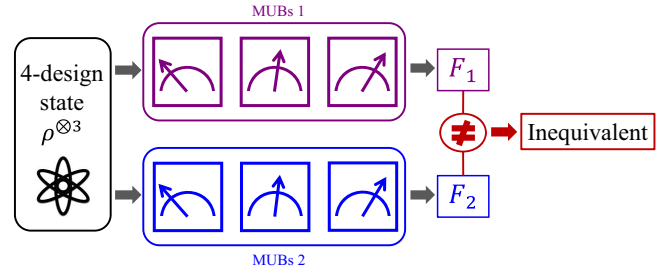


FIG. 1. The basic idea for distinguishing inequivalent triples of MUBs. After preparing three copies of each state  $\rho$  in a given 4-design and performing three projective measurements associated with each triple of MUBs, the fidelity between the optimal estimator  $\hat{\rho}$  and  $\rho$  is evaluated. The estimation fidelity of each MUB is determined by averaging the fidelity  $\text{tr}(\rho \hat{\rho})$  over the 4-design and many repetitions. Two MUBs are inequivalent if their estimation fidelities are different.

understanding elementary quantum measurements, including characterizing projective measurements, symmetric informationally complete measurements, and MUBs, distinguishing inequivalent symmetric informationally complete measurements and MUBs, and demonstrating quantum incompatibility [33].

In the above analysis, the ensemble of Haar random pure states can be replaced by any ensemble of pure states that forms a  $t$ -design with  $t = N + 1$ , which might be more appealing to practical applications. Recall that a set of  $K$  states  $\{|\psi_j\rangle\}_j$  in  $\mathcal{H}$  is a  $t$ -design if the operator  $\sum_j (|\psi_j\rangle\langle\psi_j|)^{\otimes t}$  is proportional to the projector  $P_t$  onto the symmetric subspace in  $\mathcal{H}^{\otimes t}$  [37–39].

*Distinguishing inequivalent MUBs.*—Here, we are particularly interested in inequivalent triples of MUBs in dimension 4, which can be distinguished by the three-copy estimation fidelity [33] as illustrated in Fig. 1. The three bases are denoted by  $\{|\alpha_j\rangle\}_j$ ,  $\{|\beta_j\rangle\}_j$ , and  $\{|\gamma_j\rangle\}_j$ , respectively, where  $j = 1, 2, 3, 4$ ; the corresponding rank-1 projective measurements read  $\mathcal{A} = \{|\alpha_j\rangle\langle\alpha_j|\}_j$ ,  $\mathcal{B} = \{|\beta_j\rangle\langle\beta_j|\}_j$ , and  $\mathcal{C} = \{|\gamma_j\rangle\langle\gamma_j|\}_j$ . To be specific, the first basis is chosen as the computational basis; the second and third bases correspond to the columns of the two Hadamard matrices, respectively [27,33]:

$$\begin{aligned} H_{\mathcal{B}} &= \frac{1}{2} \begin{pmatrix} 1 & 1 & 1 & 1 \\ 1 & ie^{ix} & -1 & -ie^{ix} \\ 1 & -1 & 1 & -1 \\ 1 & -ie^{ix} & -1 & ie^{ix} \end{pmatrix}, \\ H_{\mathcal{C}} &= \frac{1}{2} \begin{pmatrix} 1 & 1 & 1 & 1 \\ -e^{iy} & e^{iz} & e^{iy} & -e^{iz} \\ 1 & -1 & 1 & -1 \\ e^{iy} & e^{iz} & -e^{iy} & -e^{iz} \end{pmatrix}, \end{aligned} \quad (3)$$

where  $x, y, z \in [0, \pi]$  are three real parameters. By construction, it is easy to verify that

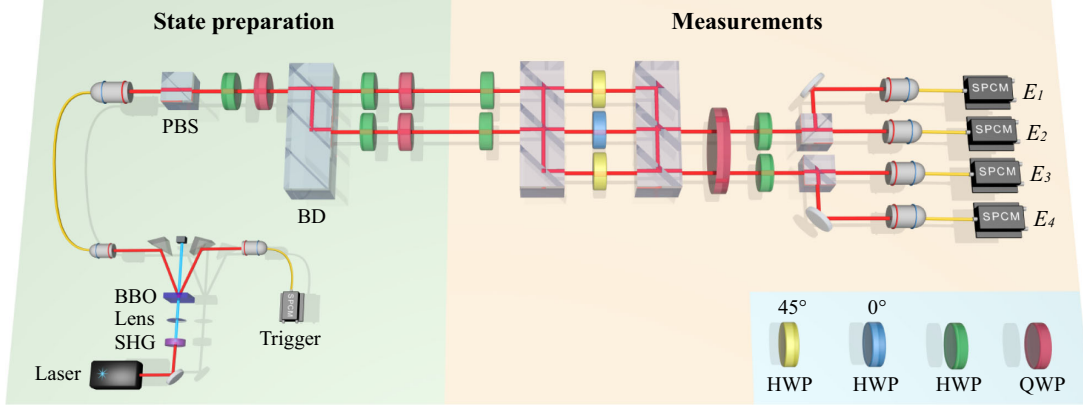


FIG. 2. Experimental setup. The module of state preparation generates a heralded single photon using the type-II beamlike phase-matched spontaneous parametric down-conversion process and prepares the desired ququad state in polarization and path degrees of freedom. The measurement module implements one of the three projective measurements  $\mathcal{A}$ ,  $\mathcal{B}$ , and  $\mathcal{C}$  associated with a triple of MUBs. The four detectors at positions  $E_1$  to  $E_4$  correspond to the four outcomes of the measurement. Key elements include polarizing beam splitters (PBSs), half wave plates (HWPs), quarter wave plates (QWPs), and beam displacers (BDs). The wave plates without angles specified are subject to rotations during the experiments.

$$|\langle \alpha_j | \beta_k \rangle|^2 = |\langle \beta_k | \gamma_l \rangle|^2 = |\langle \alpha_j | \gamma_l \rangle|^2 = \frac{1}{4} \quad (4)$$

for  $j, k, l = 1, 2, 3, 4$ . So the three bases for given  $x, y, z$  are indeed mutually unbiased. As shown in Ref. [33], the estimation fidelity  $F_{\text{MUB}}(x, y, z) := F(\mathcal{A} \otimes \mathcal{B} \otimes \mathcal{C})$  can be used to distinguish inequivalent MUBs. Moreover, the difference between the maximum and minimum estimation fidelities is about 4.1%, which is amenable to experimental demonstration.

To determine the estimation fidelity in experiments, we prepare three copies of each ququad state  $\rho_i$  from a given 4-design composed of  $K$  states and perform the three projective measurements  $\mathcal{A}$ ,  $\mathcal{B}$ , and  $\mathcal{C}$ , respectively. If the outcomes  $j, k, l$  are obtained, then we construct an estimator  $\hat{\rho}_{jkl}$  on the eigenspace of  $\mathcal{Q}(|\alpha_j\rangle\langle\alpha_j| \otimes |\beta_k\rangle\langle\beta_k| \otimes |\gamma_l\rangle\langle\gamma_l|)$  corresponding to the largest eigenvalue and evaluate its fidelity with  $\rho_i$ . To suppress statistical fluctuation, the same measurements are repeated  $M$  times for each state  $\rho_i$  in the 4-design. Denote by  $\hat{\rho}_{im}$  the  $m$ th estimator for the  $i$ th state  $\rho_i$ , where  $m = 1, 2, \dots, M$  and  $i = 1, 2, \dots, K$ . Then the estimation fidelity is calculated as follows:

$$F_{\text{MUB}}(x, y, z) = \frac{1}{KM} \sum_i \sum_m \text{tr}(\rho_i \hat{\rho}_{im}). \quad (5)$$

To facilitate experimental realization, we constructed two 4-designs with small cardinalities in dimension 4. The first 4-design is constructed from an orbit of length 960 of the restricted Clifford group and is referred to as the *Clifford 4-design* henceforth. By contrast, the full Clifford orbit has length 3840 (see Secs. S1 and S2 in the Supplemental Material [40]). This theoretical result is of independent interest, given that the Clifford group is

only a 3-design, and the restricted Clifford group is only a 2-design [43–46]. The second one is a (approximate) *numerical 4-design* composed of 200 states, which is generated using the optimization algorithm in Refs. [47,48] (see Sec. S3 in the Supplemental Material [40]).

*Experimental setup.*—The experimental setup for realizing the three-copy estimation protocol is illustrated in Fig. 2. We use the polarization (horizontal  $H$  and vertical  $V$ ) and path (up and down) degrees of freedom of a single photon to form a ququad. The setup is composed of two modules: the state preparation module, which can generate an arbitrary ququad state, and the measurement module, which can perform one of the projective measurements  $\mathcal{A}$ ,  $\mathcal{B}$ , and  $\mathcal{C}$ .

In the state preparation process, a light pulse from a Ti-sapphire laser centered around 780 nm, with a repetition rate of 76.11 MHz and pulse duration of about 150 fs, passes through a frequency doubler. Then the 12 mW up-converted ultraviolet pulse is focused onto a BBO crystal cut for the type-II beamlike phase-matched spontaneous parametric down-conversion process to create a pair of degenerate noncollinear photons [49]. One photon is detected by a single-photon-counting module as a trigger, while the other acts as a heralded single-photon source. The heralding efficiency is approximately 15%. The twofold coincidence rate is about 11 000 counts per second. The single photon is initialized in  $H$  polarization by a polarizing beam splitter (PBS). Any polarization state can be prepared by a combination of a half-wave plate (HWP) and a quarter-wave plate (QWP). A beam displacer (BD) that separates the  $H$  component and  $V$  component by 4 mm allows us to produce a bipartite state of polarization and path, where each photon has certain probability to be in one of those paths, relying on the incoming polarization state. The following two combinations of HWPs and QWPs adjust

TABLE I. Overall fidelity of the measurement  $\mathcal{C}(y, z)$  realized in the experiment. Each fidelity value is the average over ten repeated reconstructions, and the error bar indicates the standard deviation over the ten repetitions.

$z$	0	$\pi/8$	$\pi/4$	$3\pi/8$	$\pi/2$	$5\pi/8$	$3\pi/4$	$7\pi/8$	$\pi$
$\mathcal{C}(y = \pi/2)$	0.9979(2)	0.9966(4)	0.9943(12)	0.9962(8)	0.9975(8)	0.9966(10)	0.9948(8)	0.9956(7)	0.9975(4)
$\mathcal{C}(y = 0)$	0.9977(3)	0.9965(7)	0.9938(10)	0.9959(10)	0.9976(2)	0.9954(12)	0.9939(7)	0.9947(10)	0.9978(4)

the polarization states in the two paths so as to generate the desired ququad state.

Then, the state is sent into the measurement module, which performs one of the projective measurements  $\mathcal{A}$ ,  $\mathcal{B}$ , and  $\mathcal{C}$  (see Sec. S4 in the Supplemental Material [40]). The regulation of the parameters  $x, y, z$  featuring in  $\mathcal{B}$  and  $\mathcal{C}$  is realized by changing the rotation angles of some HWPs. Four single-photon-counting modules at the end correspond to four outcomes of the measurement. The phase stability of the interferometers is checked and recalibrated every 2 h by an automatic control program.

*Experimental results.*—In our experiment, we considered 18 triples of MUBs corresponding to the parameters  $x = \pi/2$ ,  $y \in \{0, \pi/2\}$ , and  $z \in \{0, \pi/8, \pi/4, \dots, \pi\}$ , which share the two bases  $\mathcal{A}$  and  $\mathcal{B}(x = \pi/2)$ . To characterize each projective measurement that was actually realized, we sent 36 states, the tensor products of the six eigenstates of three Pauli operators, to the measurement device and performed quantum measurement tomography. Each state was prepared and measured 10 000 times. Then the four projectors were reconstructed from the measurement statistics using the method in Ref. [50] and the overall fidelity was evaluated as in Ref. [51]. This procedure was repeated ten times to determine the mean fidelity and error bar (standard deviation). Overall fidelities of the realized measurements for  $\mathcal{A}$  and  $\mathcal{B}(x = \pi/2)$  are  $0.9990 \pm 0.0001$  and  $0.9977 \pm 0.0003$ , respectively, while those for  $\mathcal{C}(y, z)$  are shown in Table I. The average overall fidelity of these measurements is above 0.995, demonstrating that they were realized with high quality.

Next, we implemented the three-copy estimation protocol to determine the estimation fidelity  $F_{\text{MUB}}(x, y, z)$ . To this end, we prepared three copies of each state in the Clifford 4-design and performed the three projective measurements  $\mathcal{A}$ ,  $\mathcal{B}(x = \pi/2)$ , and  $\mathcal{C}(y, z)$ , respectively. To suppress statistical fluctuation and determine the error bar, the preparation and measurement procedure were repeated  $10\,000 \times 10$  times. For simplicity, we share the measurement outcomes of  $\mathcal{A}$  and  $\mathcal{B}(x = \pi/2)$  for all 18 sets of MUBs. The estimation fidelity  $F_{\text{MUB}}(x, y, z)$  calculated by Eq. (5) is shown in plot (a) in Fig. 3. The experimental results (circles with error bars) coincide well with the theoretical predictions (solid lines). This claim is further corroborated by Table II, which shows the average and maximum deviations between experiments and theory. The experimental errors mainly come from the instability and drift of the phases of the Mach-Zehnder

interferometers. Figure 3 clearly delineates the variation of the estimation fidelity with the parameters  $y, z$  for  $x = \pi/2$ , which highlights the operational distinctions between inequivalent MUBs. Notably, the estimation fidelity reaches the maximum 0.5197 at  $x = y = z = \pi/2$  and the minimum 0.4992 at  $x = \pi/2$ ,  $y = 0$ ,  $z = \pi$ ; the difference 0.0205 is 25 times larger than the average deviation shown in Table II.

Next, we implemented the three-copy estimation protocol based on the numerical 4-design instead of the Clifford 4-design. The results shown in plot (b) in Fig. 3 and Table II are quite similar to the counterparts based on the Clifford 4-design, although the two 4-designs are very different. These results further demonstrate that the operational distinctions between inequivalent MUBs are independent of the choice of 4-designs. Incidentally, inequivalent triples of MUBs in dimension 4 cannot be distinguished by noise

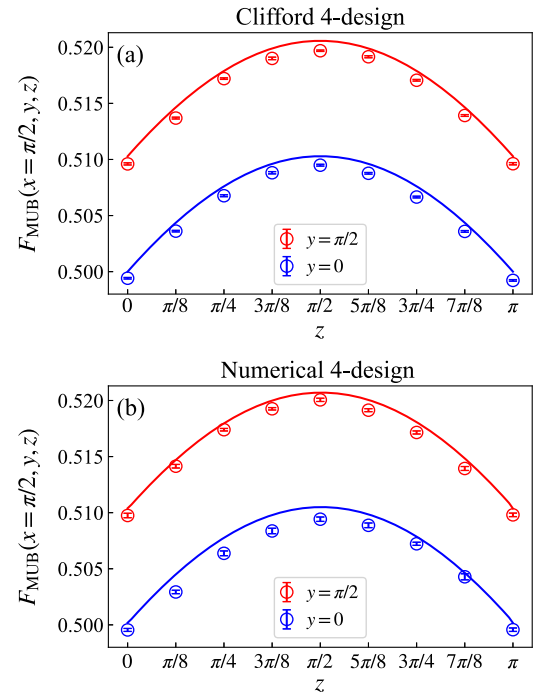


FIG. 3. Experimental results (circles with error bars) and theoretical predictions (solid lines) on the three-copy estimation fidelity  $F_{\text{MUB}}(x, y, z) = F(\mathcal{A} \otimes \mathcal{B} \otimes \mathcal{C})$  based on the Clifford 4-design (a) and numerical 4-design (b), respectively. The error bars indicate the standard deviations over ten repeated experiments.



TABLE II. Average and maximum deviations between experimental (three-copy and two-copy) estimation fidelities and theoretical predictions based on the Clifford 4-design and numerical 4-design, respectively.

	4-design	Average	Maximum
Three copy	Clifford	0.0008	0.0010
	Numerical	0.0008	0.0016
Two copy	Clifford	0.0007	0.0013
	Numerical	0.0009	0.0019

robustness considered in Ref. [31], which manifests the advantage of our approach.

As a comparison, the two-copy estimation fidelity achieved by any product measurement based on MUBs equals 0.4667 [33], assuming that the state ensemble forms an ideal 4-design. Note that inequivalent MUBs cannot be distinguished by the two-copy estimation fidelity, which provides information only about pairwise overlaps of the basis states [33]. To demonstrate this result, we reprocessed the experimental data to determine the two-copy estimation fidelity. The experimental two-copy estimation fidelities achieved by  $\mathcal{A} \otimes \mathcal{B}(x = \pi/2)$  are  $0.4664 \pm 0.0001$  and  $0.4668 \pm 0.0001$  based on the Clifford 4-design and numerical 4-design, respectively, while those for  $\mathcal{A} \otimes \mathcal{C}$

and  $\mathcal{B} \otimes \mathcal{C}$  are shown in Fig. 4 together with theoretical predictions. The average and maximum deviations are shown in Table II. Again, the experimental results agree very well with theoretical predictions even if the numerical 4-design is not ideal.

*Summary.*—In this work, we implemented a three-copy estimation protocol to demonstrate the operational distinctions between inequivalent triples of MUBs. In our experiments, we used polarization and path degrees of freedom of a photon to form a ququad and performed projective measurements associated with 18 triples of MUBs in dimension 4 with high quality. The experimental estimation fidelities agree well with theoretical predictions with only 0.16% average deviation, which is accurate enough to distinguishing inequivalent MUBs. Our experiments clearly demonstrate that inequivalent MUBs may have different information-extraction capabilities, which have operational consequences. These results are of intrinsic interest not only to foundational studies, but also to many tasks in quantum information processing, such as quantum state estimation, entanglement detection, and quantum communication. In the future, it would be interesting to explore the operational distinctions between inequivalent pairs of MUBs and inequivalent MUBs in higher dimensions.

The work at the University of Science and Technology of China is supported by the National Natural Science Foundation of China (Grants No. 62222512, No. 12104439, No. 12134014, and No. 11974335), the Anhui Provincial Natural Science Foundation (Grant No. 2208085J03), the Innovation Program for Quantum Science and Technology (Grant No. 2021ZD0301202), USTC Research Funds of the Double First-Class Initiative (Grants No. YD2030002007 and No. YD2030002011) and the Fundamental Research Funds for the Central Universities (Grant No. WK2470000035). The work at Fudan University is supported by the National Natural Science Foundation of China (Grant No. 92165109), National Key Research and Development Program of China (Grant No. 2022YFA1404204), and Shanghai Municipal Science and Technology Major Project (Grant No. 2019SHZDZX01).

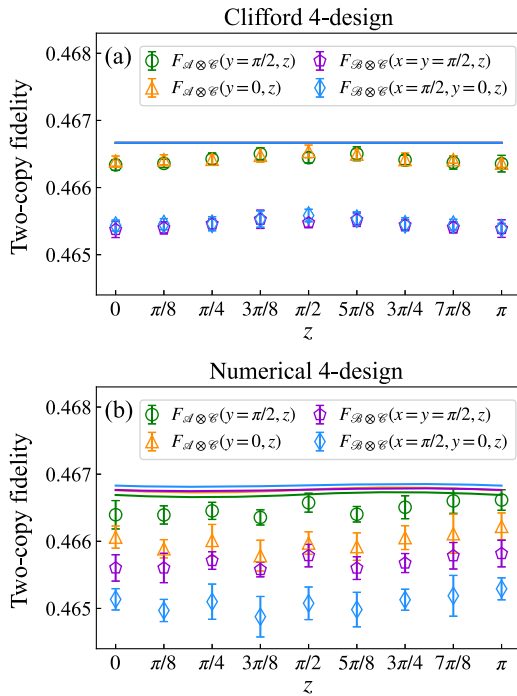


FIG. 4. Experimental results (markers with error bars) and theoretical predictions (solid lines) on the two-copy estimation fidelities achieved by the product measurements  $\mathcal{A} \otimes \mathcal{C}$  and  $\mathcal{B} \otimes \mathcal{C}$  based on the Clifford 4-design (a) and numerical 4-design (b), respectively. The error bars indicate the standard deviations over ten repeated experiments.

\*These authors contributed equally to this work.

†houzhibo@ustc.edu.cn

‡zhuhuanjun@fudan.edu.cn

§gyxiang@ustc.edu.cn

- [1] J. von Neumann, *Mathematical Foundations of Quantum Mechanics* (Princeton University Press, Princeton, 2018), translated from the German edition by R. T. Beyer.
- [2] M. A. Nielsen and I. L. Chuang, *Quantum Computation and Quantum Information: 10th Anniversary Edition* (Cambridge University Press, Cambridge, UK, 2010).

- [3] P. Busch, P.J. Lahti, J.-P. Pellonpää, and K. Ylino, *Quantum Measurement* (Springer, Cham, 2016).
- [4] J. Schwinger, Unitary operator bases, *Proc. Natl. Acad. Sci. U.S.A.* **46**, 570 (1960).
- [5] I.D. Ivonovic, Geometrical description of quantal state determination, *J. Phys. A: Math. Gen.* **14**, 3241 (1981).
- [6] W.K. Wootters and B.D. Fields, Optimal state-determination by mutually unbiased measurements, *Ann. Phys. (N.Y.)* **191**, 363 (1989).
- [7] T. Durt, B.-G. Englert, I. Bengtsson, and K. Życzkowski, On mutually unbiased bases, *Int. J. Quantum. Inform.* **08**, 535 (2010).
- [8] N. Bohr, The quantum postulate and the recent development of atomic theory, *Nature (London)* **121**, 580 (1928).
- [9] W. Heisenberg, Über den anschaulichen inhalt der quantentheoretischen kinematik und mechanik, *Z. Phys.* **43**, 172 (1927).
- [10] H.P. Robertson, The uncertainty principle, *Phys. Rev.* **34**, 163 (1929).
- [11] P. Busch, P. Lahti, and R.F. Werner, Colloquium: Quantum root-mean-square error and measurement uncertainty relations, *Rev. Mod. Phys.* **86**, 1261 (2014).
- [12] S. Wehner and A. Winter, Entropic uncertainty relations—a survey, *New J. Phys.* **12**, 025009 (2010).
- [13] P.J. Coles, M. Berta, M. Tomamichel, and S. Wehner, Entropic uncertainty relations and their applications, *Rev. Mod. Phys.* **89**, 015002 (2017).
- [14] C.H. Bennett and G. Brassard, Quantum cryptography: Public key distribution and coin tossing, in *Proceedings of the IEEE International Conference on Computers, Systems, and Signal Processing*, Bangalore, India (IEEE, New York, 1984), p. 175.
- [15] D. Mayers and A. Yao, Quantum cryptography with imperfect apparatus, in *Proceedings 39th Annual Symposium on Foundations of Computer Science* (1998), pp. 503–509.
- [16] A. Tavakoli, M. Farkas, D. Rosset, J.-D. Bancal, and J. Kaniewski, Mutually unbiased bases and symmetric informationally complete measurements in Bell experiments, *Sci. Adv.* **7**, eabc3847 (2021).
- [17] E.A. Aguilar, J.J. Borkala, P. Mironowicz, and M. Pawłowski, Connections between mutually unbiased bases and quantum random access codes, *Phys. Rev. Lett.* **121**, 050501 (2018).
- [18] M. Farkas and J. Kaniewski, Self-testing mutually unbiased bases in the prepare-and-measure scenario, *Phys. Rev. A* **99**, 032316 (2019).
- [19] A. Roy and A.J. Scott, Weighted complex projective 2-designs from bases: Optimal state determination by orthogonal measurements, *J. Math. Phys. (N.Y.)* **48**, 072110 (2007).
- [20] H. Zhu, Quantum state estimation with informationally overcomplete measurements, *Phys. Rev. A* **90**, 012115 (2014).
- [21] R.B.A. Adamson and A.M. Steinberg, Improving quantum state estimation with mutually unbiased bases, *Phys. Rev. Lett.* **105**, 030406 (2010).
- [22] Z. Li, Y.-G. Han, and H. Zhu, Efficient verification of bipartite pure states, *Phys. Rev. A* **100**, 032316 (2019).
- [23] H. Zhu and M. Hayashi, Optimal verification and fidelity estimation of maximally entangled states, *Phys. Rev. A* **99**, 052346 (2019).
- [24] G. Tóth and O. Gühne, Detecting genuine multipartite entanglement with two local measurements, *Phys. Rev. Lett.* **94**, 060501 (2005).
- [25] J. Bavaresco, N. Herrera Valencia, C. Klöckl, M. Pivoluska, P. Erker, N. Friis, M. Malik, and M. Huber, Measurements in two bases are sufficient for certifying high-dimensional entanglement, *Nat. Phys.* **14**, 1032 (2018).
- [26] J. Bae, A. Bera, D. Chruściński, B.C. Hiesmayr, and D. McNulty, How many mutually unbiased bases are needed to detect bound entangled states?, *J. Phys. A: Math. Theor.* **55**, 505303 (2022).
- [27] S. Brierley, S. Weigert, and I. Bengtsson, All mutually unbiased bases in dimensions two to five, *Quantum Inf. Comput.* **10**, 803 (2009).
- [28] T. Paterek, B. Dakić, and Č. Brukner, Mutually unbiased bases, orthogonal latin squares, and hidden-variable models, *Phys. Rev. A* **79**, 012109 (2009).
- [29] W.M. Kantor, MUBs inequivalence and affine planes, *J. Math. Phys. (N.Y.)* **53**, 032204 (2012).
- [30] P. Horodecki, L. Rudnicki, and K. Życzkowski, Five open problems in quantum information theory, *PRX Quantum* **3**, 010101 (2022).
- [31] S. Designolle, P. Skrzypczyk, F. Fröwis, and N. Brunner, Quantifying measurement incompatibility of mutually unbiased bases, *Phys. Rev. Lett.* **122**, 050402 (2019).
- [32] B.C. Hiesmayr, D. McNulty, S. Baek, S. S. Roy, J. Bae, and D. Chruściński, Detecting entanglement can be more effective with inequivalent mutually unbiased bases, *New J. Phys.* **23**, 093018 (2021).
- [33] H. Zhu, Quantum measurements in the light of quantum state estimation, *PRX Quantum* **3**, 030306 (2022).
- [34] F. Bouchard, K. Heshami, D. England, R. Fickler, R.W. Boyd, B.-G. Englert, L.L. Sánchez-Soto, and E. Karimi, Experimental investigation of high-dimensional quantum key distribution protocols with twisted photons, *Quantum* **2**, 111 (2018).
- [35] Q. Zeng, B. Wang, P. Li, and X. Zhang, Experimental high-dimensional Einstein-Podolsky-Rosen steering, *Phys. Rev. Lett.* **120**, 030401 (2018).
- [36] M.J. Kewming, S. Shrapnel, A.G. White, and J. Romero, Hiding ignorance using high dimensions, *Phys. Rev. Lett.* **124**, 250401 (2020).
- [37] J.M. Renes, R. Blume-Kohout, A.J. Scott, and C.M. Caves, Symmetric informationally complete quantum measurements, *J. Math. Phys. (N.Y.)* **45**, 2171 (2004).
- [38] G. Zauner, Quantum designs: Foundations of a noncommutative design theory, *Int. J. Quantum. Inform.* **09**, 445 (2011).
- [39] A.J. Scott, Tight informationally complete quantum measurements, *J. Phys. A: Math. Gen.* **39**, 13507 (2006).
- [40] See Supplemental Material at <http://link.aps.org/supplemental/10.1103/PhysRevLett.132.080202> for the theoretical and experimental details, which includes Refs. [41,42].
- [41] B. Bolt, T.G. Room, and G.E. Wall, On the Clifford collineation, transform and similarity groups. I., *J. Aust. Math. Soc.* **2**, 60 (1961).
- [42] B. Bolt, T.G. Room, and G.E. Wall, On the Clifford collineation, transform and similarity groups. II., *J. Aust. Math. Soc.* **2**, 80 (1961).
- [43] D. Gottesman, Stabilizer codes and quantum error correction, [arXiv:quant-ph/9705052](https://arxiv.org/abs/quant-ph/9705052).

- [44] H. Zhu, Multiqubit Clifford groups are unitary 3-designs, *Phys. Rev. A* **96**, 062336 (2017).
- [45] Z. Webb, The Clifford group forms a unitary 3-design, *Quantum Inf. Comput.* **16**, 1379 (2016).
- [46] H. Zhu, R. Kueng, M. Grassl, and D. Gross, The Clifford group fails gracefully to be a unitary 4-design, [arXiv: 1609.08172](https://arxiv.org/abs/1609.08172).
- [47] D. Hughes and S. Waldron, Spherical  $(t, t)$ -designs with a small number of vectors, *Linear Algebra Appl.* **608**, 84 (2021).
- [48] A. Elzenaar, <https://github.com/aelzenaar/tightframes>.
- [49] S. Takeuchi, Beamlike twin-photon generation by use of type II parametric downconversion, *Opt. Lett.* **26**, 843 (2001).
- [50] J. Fiurášek, Maximum-likelihood estimation of quantum measurement, *Phys. Rev. A* **64**, 024102 (2001).
- [51] Z. Hou, J.-F. Tang, J. Shang, H. Zhu, J. Li, Y. Yuan, K.-D. Wu, G.-Y. Xiang, C.-F. Li, and G.-C. Guo, Deterministic realization of collective measurements via photonic quantum walks, *Nat. Commun.* **9**, 1414 (2018).